

Supporting Information for

**Thermally conductive phase change electrode for in-situ thermal
management of lithium-ion batteries**

Lu-Ning Wang, Shuang-Zhu Li, Wei-Wei Liu, Niu Jiang, Yu-Yang Song, Lu Bai, Yu

Wang, Bo Yin, Jie Yang*, Wei Yang*

College of Polymer Science and Engineering, Sichuan University, State Key
Laboratory of Polymer Materials Engineering, Chengdu 610065, Sichuan, P. R. China.

* Corresponding authors: psejieyang@scu.edu.cn (J. Yang), weiyang@scu.edu.cn (W. Yang).

Determination of battery internal resistance using a DCIR method

All experimental samples were assembled into coin cells using LiFePO_4 as cathode and Li metal as the anode for DCIR tests. The DCIR measurements were conducted *via* Neware Battery measurement system with a voltage range of 2.5 V ~ 4.2 V at 30 °C. The battery was charged and discharged successively at a multiplication rate of 0.1 C for 1 s with 10 cycles, and the interval is 10 s for each cycle from the resting state to the steady state. The voltage and current changes during the charging and discharging processes were recorded in real time, and the voltage difference was divided to obtain the internal resistance according to the current difference.

Results

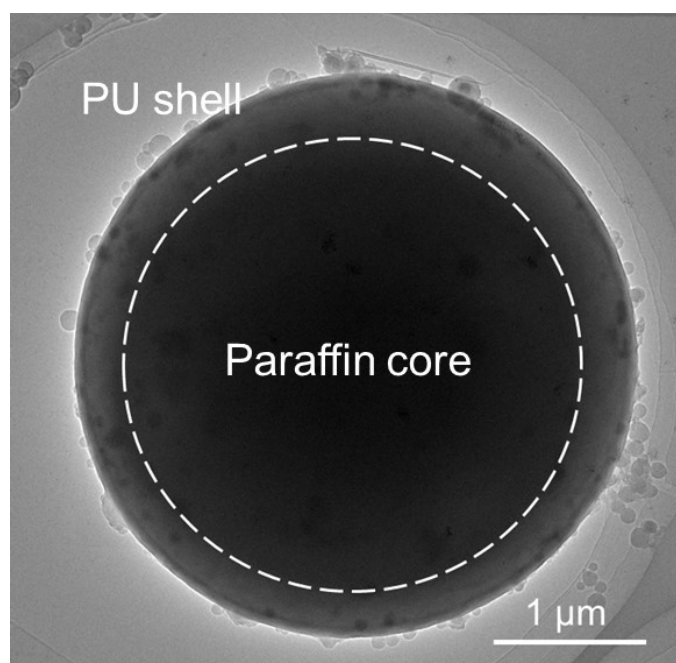


Fig. S1 TEM image of phase change microcapsules.

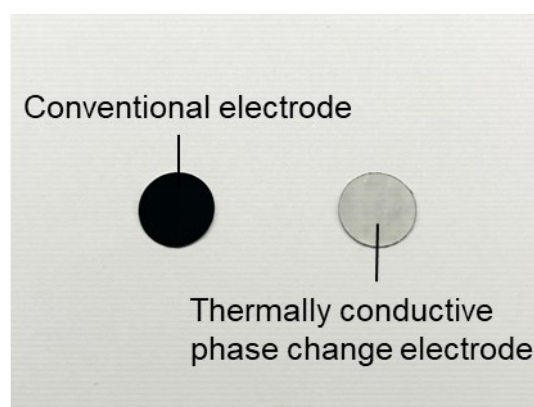


Fig. S2 Digital picture of electrodes before and after coating thermally conductive phase change

components.

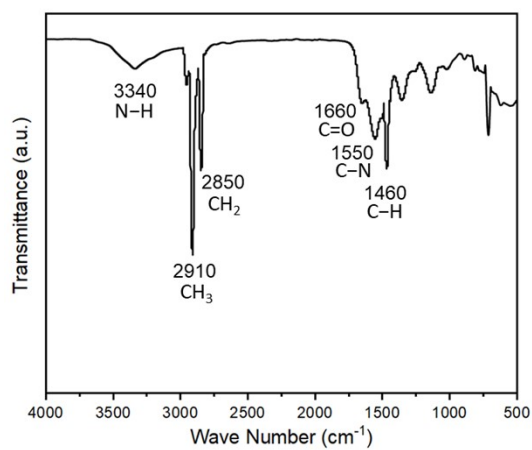


Fig. S3 FT-IR spectrum of phase change microcapsules.

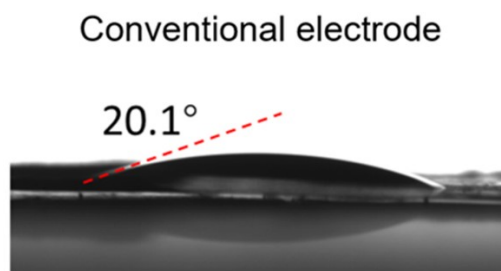


Fig. S4 Contact angle between the electrode and the electrolyte before coating thermally conductive phase change components.

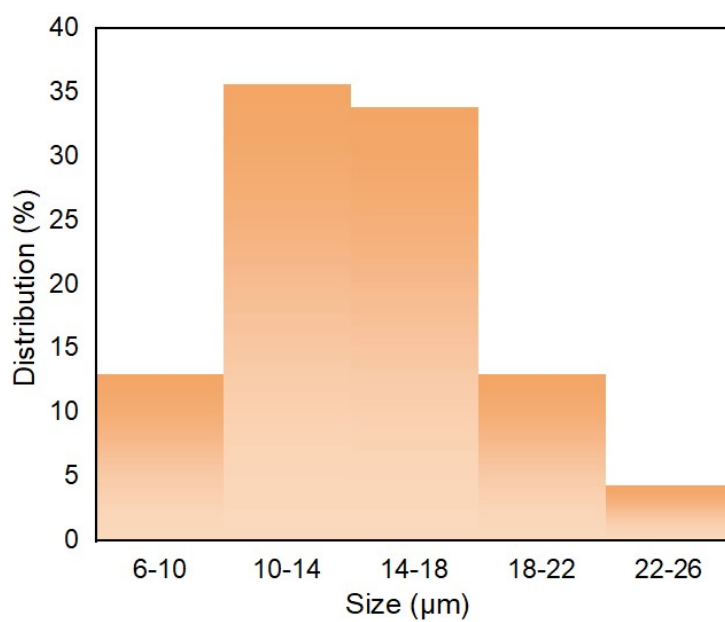


Fig. S5 Size distribution of the BN flakes used in the coating.

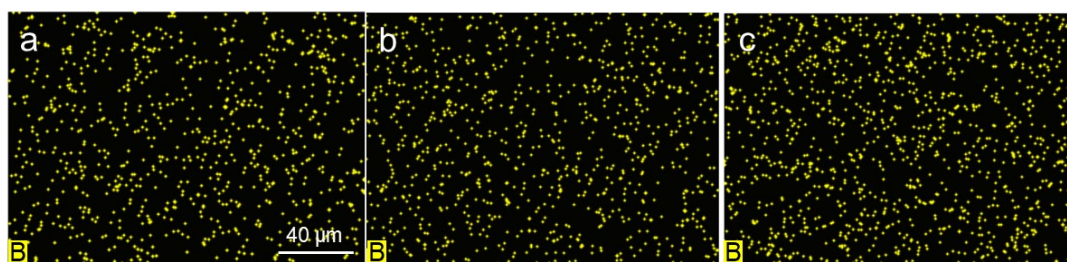


Fig. S6 EDS mapping images showing the distribution of B elements within the (a) 10BN, (b) 20BN, and (c) 30BN.

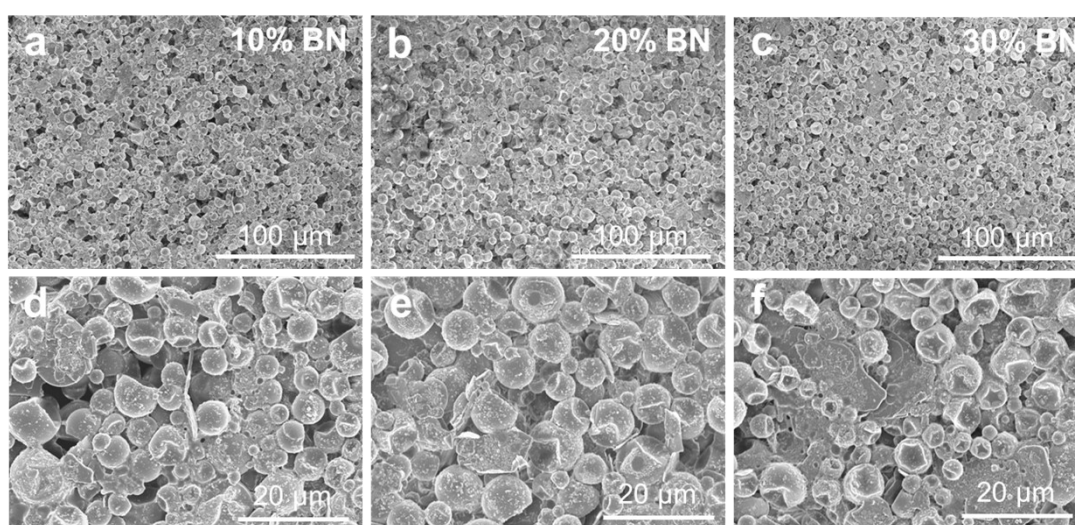


Fig. S7 SEM images of the surface of modified electrodes with the BN loadings of (a) 10 wt%, (b) 20 wt%, and (c) 30 wt%.

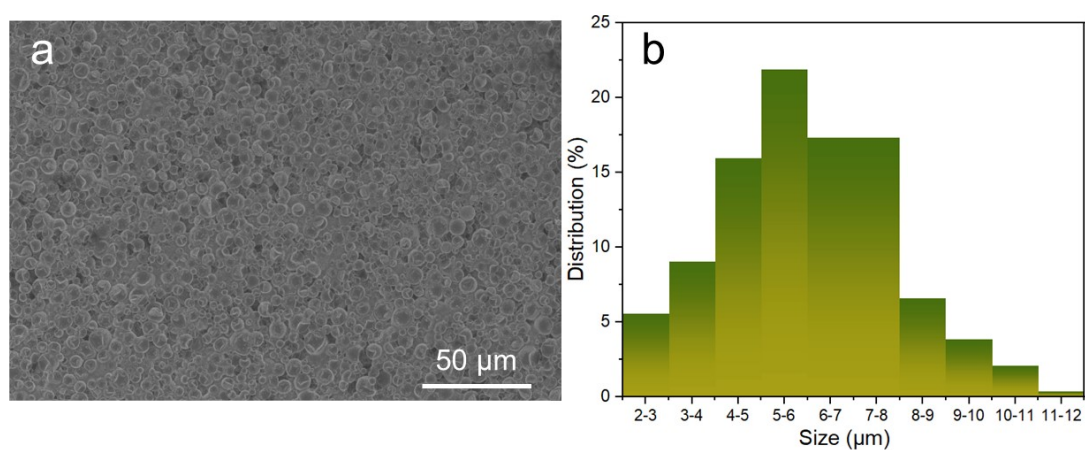


Fig. S8 (a) SEM image of the phase change electrode and (b) corresponding particle size distribution of the phase change microcapsules used in the coating.

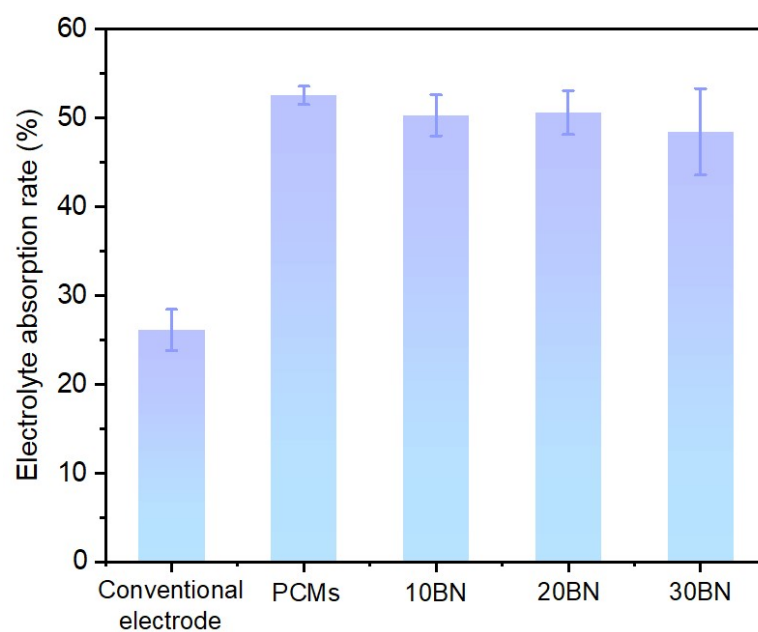


Fig. S9 Electrolyte absorption rate of conventional electrode, PCMs, 10BN, 20BN, and 30BN.

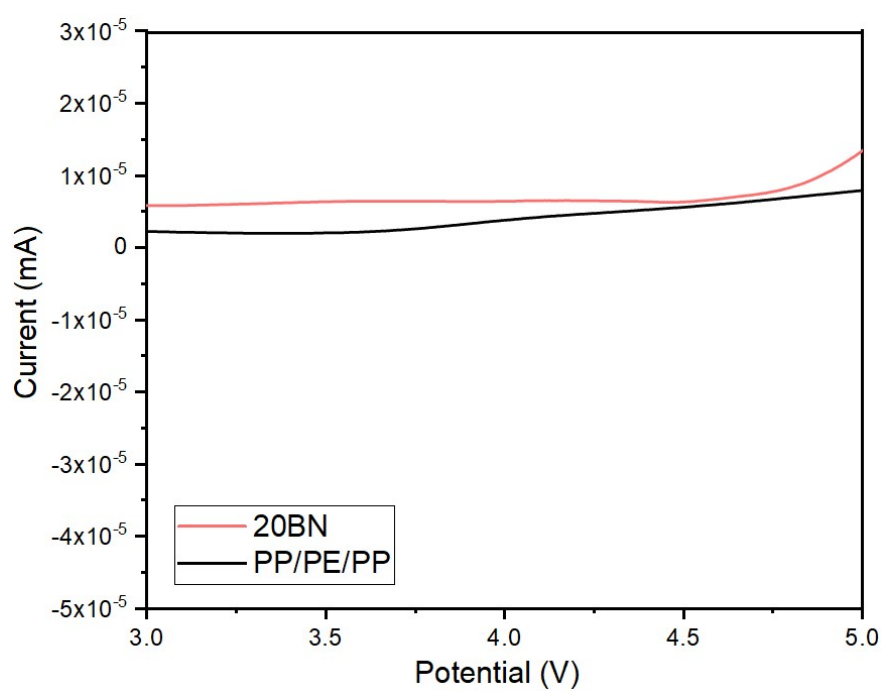


Fig. S10 LSV testing curves of the modified and normal batteries.

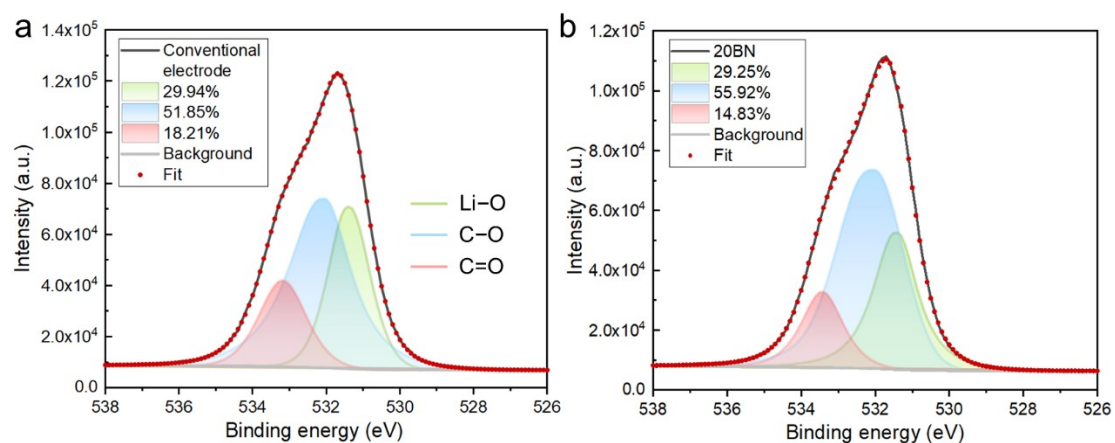


Fig. S11 O1s X-ray photoelectron spectroscopy (XPS) analysis of cycled lithium metal anodes with (a) conventional electrode and (b) 20BN.

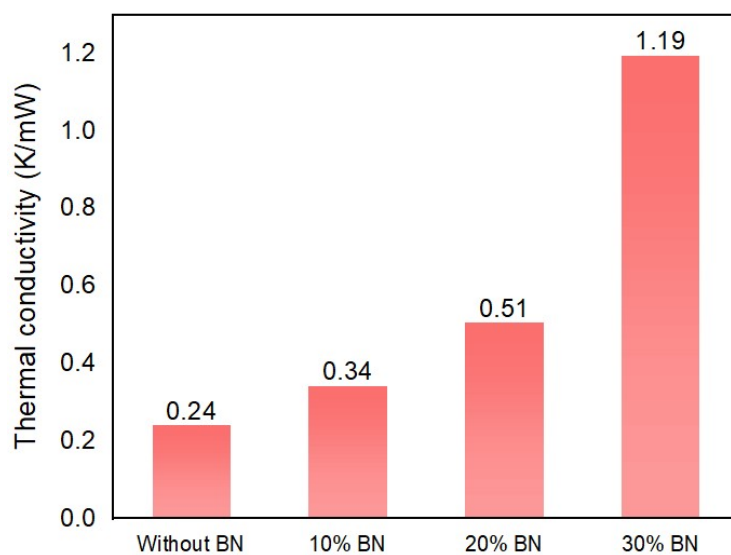


Fig. S12 Thermal conductivity of thermal management coatings without BN and with different BN loadings (10 wt%, 20 wt% and 30 wt%) at 60 °C.